VOF Simulations of Evaporation and Condensation Phenomenon Inside a Closed-Loop Thermosyphon

Vivek K. Mishra, Saroj K. Panda, Biswanath Sen, M. P. Maiya, and Dipti Samantaray

1 Introduction

The nuclear fuels prior to loading in reactors are stored in nuclear fuel storage vault. The fuels contain fissile materials, which generate decay heat during storage in the vault. Conventionally, cooling air is supplied to the vault for efficient heat removal, and the temperature inside the vault is maintained below 65 °C to maintain the integrity of the vault and ensure long-term storage of the fuel during normal operation [1]. Since it is difficult to monitor the temperature and air flow inside the vault, CFD simulations are effective to monitor these aspects of the nuclear fuel storage vault [2, 3]. Further, it is utmost important to maintain the temperature inside the vault within 90 oC during station blackout [1]. The concrete structure of the vault can degrade if the decay heat is not removed, and the longevity of the fuel storage can be affected. Therefore, an efficient passive cooling arrangement is required to effectively cool the fuels and concrete structure inside the vault.

Thermosyphon is an effective heat removal device that works on principles of both conduction and phase change. It comprises a sealed metallic tube with working fluid inside it and the heat is transferred through cyclic evaporation and condensation of working fluid. Therefore, an additional external electrical element is not required to operate the thermosyphon. Thermosyphon can be considered as a heat sink or a passive cooling system for the fuel storage vault. Therefore, it becomes important to

V. K. Mishra · D. Samantaray
Homi Bhabha National Institute, Anushaktinagar, Mumbai 400094, India

S. K. Panda · B. Sen (✉)
Indira Gandhi Centre for Atomic Research, Tamil Nadu, Kalpakkam 603102, India
e-mail: biswa@igcar.gov.in

M. P. Maiya
Department of Mechanical Engineering, Indian Institute of Technology Madras, Tamil Nadu, Chennai 600036, India

K. M. Singh et al. (eds.), *Fluid Mechanics and Fluid Power, Volume 5*, Lecture Notes in Mechanical Engineering, https://doi.org/10.1007/978-981-99-6074-3_5

study the temperature and mass transfer distribution during steady state operation in an environment which is replica of fuel storage vault.

2 Literature Review and Objective

The multiphase liquid–vapor phase change process has been investigated by different researchers using volume-of-fluid (VOF) approach, level set (LS), and combination of both the methods. The initial CFD simulations of boiling using VOF method were conducted by Schepper et al. [4]. The simulations investigated the boiling of hydrocarbon in a steam cracker. The results simulated using VOF approach were in good agreement with their previously obtained experimental data [5]. Further studies [6–10] on the simulation of boiling paved way for research and analysis of heat pipes using CFD. A wickless heat pipe also known as thermosyphon is widely used due to its passive cooling applications, reliability, cost-effectiveness and ease of manufacturing. The effect of heat flux and filling ratio on a thermosyphon which used water as a working fluid was investigated using experiments and simulations by Alizadehdakhel et al. [6]. Further, Lin et al. [7] developed a VOF-based CFD model which was able to correctly predict the thermal conductivity using temperature at evaporator and condenser end along with heat load. The miniature oscillating heat pipe using water as a working fluid. The effect of evaporator length and inner diameter of the thermosyphon was varied to analyze its heat transfer characteristics in terms of thermal conductivity. Jeong et al. [8] proposed a hybrid thermosyphon to extract heat from a spent fuel storage facility to avoid thermal degradation and maintain its structural integrity for long-term storage of spent fuel.

With the increased requirement of safety in nuclear power plants and maturity in design, the application of thermosyphon in nuclear plant is important. In a study of nuclear reactor similar to Fukushima No 1 plant, Mochizuki et al. [10] investigated the effect of a loop heat pipe to remove the residual heat from the reactor for its safe shutdown. Xiong et al. [11] experimentally studied a heat pipe for effectively removing heat from a spent fuel storage vault during an accident.

In the present study, a thermosyphon is suggested as a passive cooling system for dry storage of a nuclear fuel storage vault. The design is based on the heat generated by the storage vault. To evaluate the performance of the thermosyphon, experiments were performed to obtain thermal conductivity. In addition to this, CFD simulation of a wickless heat pipe that takes into account every aspect of the heat transfer phenomena occurring inside the heat pipe which has also been reported. CFD models can also reduce the quantity of experimentation. Therefore, in this paper, a thorough CFD modeling of two-phase flow and heat transfer processes during the operation of a straight thermosyphon has been undertaken.

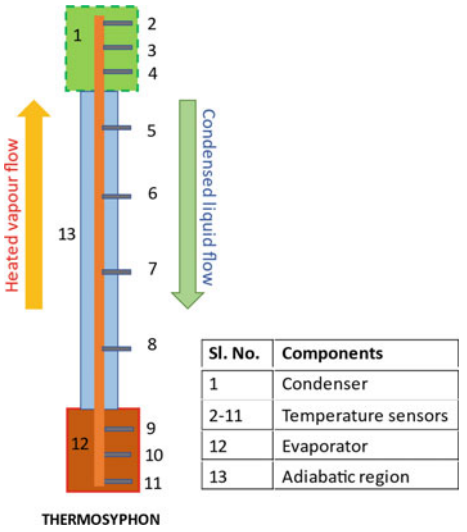

Sl. No.	Components
1	Condenser
2-11	Temperature sensors
12	Evaporator
13	Adiabatic region

Fig. 1 Schematic representation of experimental setup

3 Experimental

3.1 Experimental Setup

The schematics of the experimental apparatus for our present investigation is shown in Fig. 1. The thermosyphon was manufactured using a 2 m long copper tube with 0.022 m outer diameter, and 0.001 m of thickness. The evaporator where the heating is provided is 0.3 m long and the condenser section through which heat is dissipated is 0.2 m in length. The heat is provided to the evaporator using ceramic heaters. The condenser side is exposed to the environment to obtain natural cooling. In the middle, adiabatic region of 1.5 m length is insulated using insulation of glass wool and fiberglass cloth. The temperature is measured using thermocouples attached to the surface of the thermosyphon.

3.2 Experimental Procedure

Before initiation of the experiment, the vacuum pump is connected to the thermosyphon. The vacuum created removes the non-condensable gases and reduces the vapor pressure inside the tube. The working fluid (water) is filled in the thermosyphon and the volume of filled water is carefully measured. The pressure gauge connected to the thermosyphon indicates the pressure in the tube. A constant temperature is maintained at the evaporator end using the heater. The reading was taken around

1.5 h after achieving a stable temperature at the thermosyphon. The experiment was repeated to confirm the correctness of the experimental data.

4 Numerical Methods

4.1 Governing Equations

The two-phase flow and phase change in the thermosyphon is modeled using VOF multiphase models. The mass, momentum, and energy equations for multiphase VOF model are calculated as.

Mass conservation equation:

$$\frac{\partial(\alpha\rho)}{\partial t} + \nabla.(\alpha\rho\overline{u}) = M_s \tag{1}$$

Momentum conservation equation:

$$\frac{\partial(\rho\overline{u})}{\partial t} + \nabla.(\rho\overline{uu}) = -\nabla p + \nabla.[\mu(\nabla\overline{u} + \nabla u^T)] + \rho g + S \tag{2}$$

Energy conservation equation:

$$\frac{\partial(\rho e)}{\partial t} + \nabla.[(\rho e + p)\overline{u}] = -\nabla(k\nabla T) + S_H \tag{3}$$

where density (ρ) of liquid phase is a function of temperature, which is given as

$$\rho = 859 + 1.252T - 0.00264T^2 \tag{4}$$

The surface tension varies with the temperature and is represented as

$$\sigma = 0.098 - 1.845 \times 10^{-5}T - 2.3 \times 10^{-7}T \tag{5}$$

The equation for turbulent kinetic energy (k) is defined as

$$\begin{aligned} &\frac{\partial k}{\partial t} + \frac{\partial\left(\overline{u}_j k\right)}{\partial x_j} = \frac{\partial}{\partial x_j}\left[\left(\nu + \frac{\nu_t}{\sigma_k}\right)\frac{\partial k}{\partial x_j}\right] + \\ &\left[\nu_t\left(\frac{\partial\overline{u}_i}{\partial x_j} + \frac{\partial\overline{u}_j}{\partial x_i}\right) - \frac{2}{3}k\delta_{ij}\right]\frac{\partial\overline{u}_i}{\partial x_j} - \varepsilon \end{aligned} \tag{6}$$

The specific rate of dissipation (ε) equation is defined using

$$\frac{\partial \varepsilon}{\partial t} + \frac{\partial \left(\overline{u}_j \varepsilon\right)}{\partial x_j} = \frac{\partial}{\partial x_j}\left[\left(\nu + \frac{\nu_t}{\sigma_\varepsilon}\right)\frac{\partial \varepsilon}{\partial x_j}\right] + c_1 \frac{\varepsilon}{k}$$
$$\left[\nu_t\left(\frac{\partial \overline{u}_i}{\partial x_j} + \frac{\partial \overline{u}_j}{\partial x_i}\right) - \frac{2}{3}k\delta_{ij}\right]\frac{\partial \overline{u}_i}{\partial x_j} - c_2 \frac{\varepsilon^2}{k} \tag{7}$$

The eddy/turbulent viscosity (μ_t) was calculated using $\mu_t = \rho C_\mu \frac{k^2}{\varepsilon}$, where $C_1 = 1.44$; $C_2 = 1.92$; $C_\mu = 0.09$; $\sigma_k = 1$ and $\sigma_\varepsilon = 1.3$

4.2 Geometry and Boundary Conditions

The 2D model is built using ANSYS design modeler. In the fluid region, uniform and non-uniform grids are generated using "ANSYS-Meshing" module. The evaporator region of the thermosyphon is specified as constant temperature of 60 °C. The condensers are specified as 27 °C, with a heat transfer coefficient of 7 W/m^2-K. A heat flux of 0 W/m^2-K is applied to the adiabatic region of the thermosyphon. The entire evaporator region is patched with water and entire pressure of 450 mm-Hg is applied to the volume of thermosyphon.

5 Results and Discussion

The current numerical simulations were conducted on a 2D model of the thermosyphon to analyze the heat and phase change phenomenon in terms of temperature distributions along the height of thermosyphon and boiling and condensation phenomena near evaporator and condenser, respectively.

5.1 Validation

The temperature distributions along the length of the thermosyphon obtained from experiments are used to validate the numerical data. The predicted temperature distributions are compared with the experimentally obtained data (see Fig. 2) and found to be in good agreement with each other. The experimentally validated CFD model was used to carry out all further simulations.

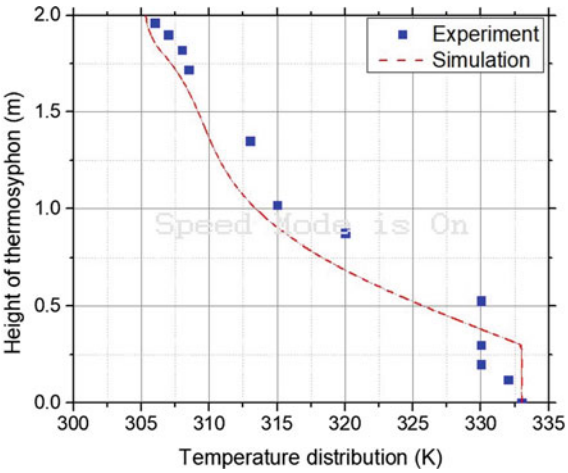

Fig. 2 Comparison of experimental measured temperature with simulated results

5.2 Temperature Distributions

The temperature contours at different time duration, during startup and steady state operation, are presented in Fig. 3. The temperature distributions inside the thermosyphon are useful to understand the heat transfer process. Initially, the operating pressure and temperature were specified as saturation values. The temperature of the evaporator was increased as the constant temperature was applied to the evaporator walls. The difference in temperature at the evaporator end leads to boiling due to heat transfer on the wall of the evaporator. The vapor flows from the evaporator to the condenser section as observed at 100 and 500 s. A heated region at the condenser is obtained at 1000 s. Later, the heat transfer process in the evaporator becomes nearly uniform.

5.3 Evaporation

The time evolution of the vapor phase obtained at the evaporator end is presented in Fig. 4. The rise of the vapor phase in the thermosyphon is responsible for heat transfer and an increase in temperature inside the thermosyphon. It is observed that initially the liquid pool is kept quiescent and the vaporization phase is reached. The vapor starts to form when the saturation temperature is reached. Further, the liquid at the top vaporizers before the liquid at the bottom. It is because the phase change is affected by the local pressure and hydrostatic pressure of the liquid. The difference in pressure at the bottom and nucleation site is difficult to be obtained. The pressure difference makes it difficult to obtain the nucleation sites in the lower region.

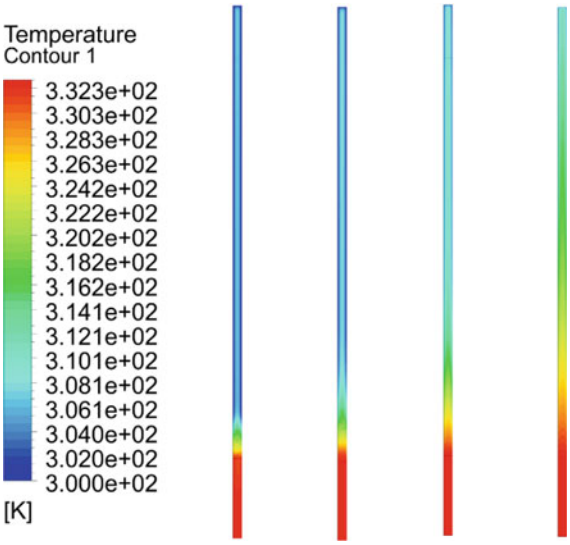

Fig. 3 Variations in temperature with time along the height of the thermosyphon

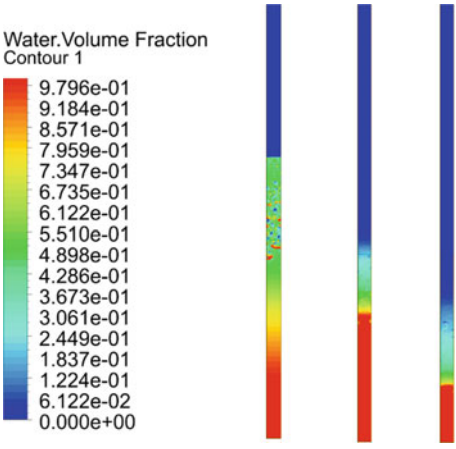

Fig. 4 Time evolution of water volume fraction distributions in the thermosyphon

5.4 Condensation of Water Film

The converse of boiling takes place at the condenser section. The condensate film obtained at the condenser and adiabatic region is presented in Fig. 5. The liquid film falls through the adiabatic region of the thermosiphon (see Fig. 5a). The liquid in the evaporator region is replenished by the continuous flow of thin liquid film as shown in Fig. 5b.

Fig. 5 Condensed water film profile near **a** condenser and **b** along the adiabatic walls

5.5 Conductivity Calculations

The resistance offered to heat transfer in the thermosyphon is calculated using the formula $R_{\text{th}} = \Delta T/Q$, where Q is the applied heat load, given as $Q = V \times I$—losses.

The thermal resistance obtained for the thermosyphon using the experiment was 0.04 K/W, whereas the thermal resistance obtained using the numerical simulation was nearly 0.034 K/W. The difference in the predicted result was obtained due to the presence of non-condensable gases in the thermosyphon and improper insulation around the thermosyphon which resulted in heat losses.

6 Conclusions

In the present study, heat and mass transport phenomena inside a two-phase closed loop thermosyphon are simulated which used water as a working fluid. The heat transfer inside the thermosyphon was due to the combined effect of conduction and phase change of the working fluid. The results of the CFD simulations show that the proposed CFD model was able to predict the temperature distribution along the length of the thermosyphon successfully. The temperature distribution inside the thermosyphon becomes uniform after 1000 s after a steady state is achieved. The boiling phenomenon in the evaporator region of the thermosyphon shows that the water boils at a higher rate near the liquid–vapor interphase due to the hydrostatic pressure difference between the two regions. The condensed liquid on the condenser wall flows through the evaporator and charges the pool of water in the evaporator. The thermal resistance was calculated to be nearly 0.38 K/W. The disparity between the experimental and numerically obtained values of the thermosyphon was due to the

presence of non-condensable gases in the tube and insufficient insulation around the thermosyphon. The present study will be helpful to understand the heat and phase change phenomenon taking place inside the thermosyphon which can be used to improve the heat removal from the fuel storage vault.

Acknowledgements One of the authors, Vivek K. Mishra, is grateful to the Department of Atomic Energy for the DGFS fellowship. All the authors thank the Engineering Services Group for their help during the commissioning of the experimental setup.

Nomenclature

e	Energy term (W)
I	Current (A)
k	Turbulence kinetic energy (m^2/s^2)
Q	Power supplied (W)
R_{th}	Thermal resistance of thermosyphon (K/W)
S	Source term (W/m^3)
T	Temperature (K)
$\overline{u}$	Supply velocity (m/s)
V	Voltage (V)
σ	Surface tension of the liquid (N/m)
ρ	Density of air (kg/m^3)
β	Coefficient of thermal expansion (1/K)
ε	Specific rate of dissipation

References

1. Design of Concrete Structures Important to Safety of Nuclear Facilities, Atomic Energy Regulatory Board, India (2001)
2. Alyokhina S (2018) Thermal analysis of certain accident conditions of dry spent nuclear fuel storage. Nucl Eng Technol 50(5):717–723
3. Mishra VK, Panda SK, Sen B, Maiya MP, Rao BPC (2022) Numerical analysis of forced convection heat transfer in a nuclear fuel storage vault. Int J Therm Sci 173:107429
4. Schepper SCKD, Heynderickx GJ, Marin GB (2009) Modeling the evaporation of a hydrocarbon feedstock in the convection section of a steam cracker. Comput Chem Eng 33(1):122–132
5. Schepper SCKD, Heynderickx GJ, Marin GB (2008) CFD modeling of all gas–liquid and vapor–liquid flow regimes predicted by the Baker chart. Chem Eng J 138(1–3):349–357
6. Alizadehdakhel M, Rahimi M, Alsairafi AA (2010) CFD Modeling of Flow and Heat Transfer in a Thermosyphon. Int Commun Heat Mass Transf 37:312–318
7. Lin Z, Wang S, Shirakashi R, Winston Zhang L (2013) Simulation of a miniature oscillating heat pipe in bottom heating mode using CFD with unsteady modelling. Int J Heat Mass Transf 57(2):642–656

8. Jeong YS, Bang IC (2016) Hybrid heat pipe based passive cooling device for spent nuclear fuel dry storage cask. Appl Therm Eng 96:277–285
9. Mochizuki M, Singh R, Nguyen T, Nguyen T (2014) Heat pipe based passive emergency core cooling system for safe shutdown of nuclear power reactor. Appl Therm Eng 73(1):699–706
10. Xiong Z, Wang M, Gu H, Ye C (2015) Experimental study on heat pipe heat removal capacity for passive cooling of spent fuel pool. Ann Nucl Energy 83:258–263